

RESEARCH

Open Access



Genomic characteristics and prognostic correlations in Chinese multiple myeloma patients

Xi Chen^{1†}, Tianchen Luo^{1†}, Wenhui Zhang^{2†}, Sheng Wang^{2†}, Mengxuan Zhu², Haiyan He¹, Jin Liu¹, Jing Lu¹, Wanting Qiang¹, Yanchun Jia¹, Nan Hou¹, Xuenan Zhao², Shan Zhang², Jing Li^{3*†} and Juan Du^{1*†}

Abstract

Background Multiple myeloma (MM) is a hematologic malignancy characterized by the proliferation of abnormal clonal plasma cells in the bone marrow. The heterogeneity in Chinese MM populations remains underexplored.

Methods We conducted whole-exome sequencing (WES) on 241 tumor samples, complemented by RNA sequencing (RNA-seq) on 131 samples from 212 Chinese MM patients.

Results We identified a novel mutational signature and analyzed molecular differences between newly diagnosed MM (NDMM) and relapsed/refractory MM (RRMM) patients. *NFKB1A* mutations were notably more frequent in NDMM patients compared to the MMRF-COMMPASS cohort (4/50 vs 22/937, $p=0.048$), with additional recurrent mutations in several genes like *TTN*, *IGLL5* and *SYNE1*. In RRMM patients, *UBR5* mutations were more prevalent (4/24 vs 0/50, $p=0.01$), alongside frequent mutations in *OBSCN*, *CACNA1H*, and *HSPG2*. Clonal evolution was assessed through multiple time points and locations, identifying genes potentially linked to circulating plasma cell formation. Cox regression analysis revealed that age and mutations in *OBSCN* and *RB1* were significant predictors of progression-free survival (PFS) in NDMM patients. Additionally, albumin, β_2 -microglobulin, and *RB1* mutations were correlated with overall survival (OS).

Conclusions In summary, we characterized the genomic landscape of MM in diverse Chinese populations, confirmed clonal evolution, and identified prognostic genes.

Keywords Multiple myeloma, Genomic characteristics, Prognosis

[†]Xi Chen, Tianchen Luo, Wenhui Zhang and Sheng Wang contributed equally to this work.

[†]Jing Li and Juan Du contributed equally to this work.

*Correspondence:

Jing Li
ljing@smmu.edu.cn
Juan Du
juan_du@live.com

¹ Department of Hematology, Myeloma & Lymphoma Center, Second Affiliated Hospital of Naval Medical University (Shanghai Changzheng Hospital), Shanghai 200003, China

² Center for Translational Medicine, Second Military Medical University, Shanghai 200433, China

³ Department of Precision Medicine, Changhai Hospital, Second Military Medical University (Naval Medical University), Shanghai 200433, China



Background

Multiple myeloma (MM) is a hematologic malignancy characterized by the presence of abnormal clonal plasma cells (PCs) in the bone marrow (BM). This malignancy exhibits significant genetic complexity and heterogeneity, driven by a multitude of genomic events that facilitate tumorigenesis and progression. Detailed cytogenetic analyses have elucidated that structural rearrangements and copy number variations (CNVs) are the predominant mechanisms underlying tumorigenesis and disease advancement [1–3]. These findings have led to the classification of MM into hierarchical subtypes: hyperdiploid (HRD) and non-hyperdiploid (non-HRD). Additional genomic events, such as further CNVs, *MYC* translocations, and somatic mutations in pathways including MAPK, NF- κ B, and DNA repair, confer selective advantages to particular subclones, thereby exacerbating disease progression. Somatic mutations, in particular, have been rigorously investigated, identifying several genes such as *KRAS*, *NRAS*, *BRAF*, and *TP53* as significantly mutated genes (SMGs) in MM, which play crucial roles in the pathogenesis of the disease [1, 4–6]. However, the spectrum of known driver events in Chinese MM populations remains limited due to constraints in available data. The unique genomic characteristics to this population are yet to be fully characterized. Additionally, most cases of newly diagnosed MM (NDMM) inevitably develop treatment resistance, progressing to relapsed/refractory MM (RRMM). Previous research has identified specific genomic features and factors that promote disease progression and affect prognosis in RRMM, offering vital insights for the development of targeted therapeutic strategies and improved disease management [7–10]. However, the genomic distinctions between NDMM and RRMM patients remain to be further elucidated.

Furthermore, MM exhibits distinct disease progression stages and often presents with multifocal tumor lesions, making it an ideal model for studying clonal evolution [11–13]. Temporally, the disease progresses from pre-malignant stages such as monoclonal gammopathy of undetermined significance (MGUS) and smoldering MM (SMM) to active MM, and then from NDMM to RRMM, indicating a clear clonal evolution pattern. Spatially, some MM patients exhibit extramedullary involvement during diagnosis and treatment, where PCs not only proliferate within the BM but also infiltrate tissues, organs, and even the peripheral blood. This observation highlights the spatial heterogeneity of MM. Therefore, investigating the clonal evolution of MM can facilitate the identification of genes associated with disease progression and extramedullary involvement, which in turn may provide promising therapeutic targets. Moreover, the current prognostic staging systems for MM are inadequate for

effectively stratifying high-risk patients, as they often overlook the biological diversity among individuals at the same stage. This variability in disease progression and treatment response highlights the need for a more refined risk assessment approach. Therefore, it is crucial to explore and validate innovative prognostic biomarkers, including genetic, epigenetic, and proteomic profiles, which can more accurately reflect disease aggressiveness and patient survival. Integrating these biomarkers into prognostic models can enhance predictions of disease progression and treatment response, facilitating personalized treatment plans for high-risk MM patients.

In this study, we performed whole-exome sequencing (WES) and RNA sequencing (RNA-seq) on 212 Chinese MM patients. We discovered a novel mutational signature specific to this population, revealing differences in mutation burden, CNVs, and recurrently mutated genes between NDMM and RRMM patients. By sampling multiple sites from the same patient over time, we traced the clonal evolution of MM. Additionally, we identified several novel candidate genes that could serve as potential prognostic markers for MM.

Methods

Patients and samples

In this study, we analyzed a Chinese MM cohort of 212 patients, encompassing 241 tumor samples, including 235 BM samples and 6 circulating plasma cell (CPC) samples, matched with 87 normal peripheral blood samples. Additionally, 15 normal blood samples from healthy individuals were collected as controls. Samples were divided into four cohorts based on sampling methods (Supplementary Figure 1). Cohort 1, named “one point & one sample,” examined the genomic features of NDMM and RRMM through single time point and site sampling. It was subdivided into discovery cohorts (1a and 1b) with 50 matched NDMM and 24 RRMM samples, and validation cohorts (1A and 1B) with 77 unmatched NDMM and 37 RRMM samples. The remaining cohorts sampled multiple time points or sites to investigate clonal evolution. Clinical data and sampling details are shown in Supplementary Table 1. Tumor samples were sorted using CD138 magnetic beads. Peripheral blood samples with a monoclonal PC ratio >5% were categorized as CPC samples, while others served as normal controls. We performed WES on all 343 samples and RNA-seq on 131 tumor samples. Sequencing and quality check data are provided in Supplementary Table 2.

Statistical analysis

We collected clinical data from 212 MM patients, including gender, age at diagnosis, M-protein type, disease stage, and FISH abnormalities. Positivity thresholds were

set at 10% for chromosomal translocations and 20% for CNVs. Statistical analyses were conducted using R v4.1.1, with $p < 0.05$ as the significance level. Continuous variables were expressed as mean \pm standard deviation for normal distributions and median with interquartile range (IQR) for non-normal distributions. The Kolmogorov–Smirnov test assessed normality and variance homogeneity. The Mann–Whitney U test compared non-normally distributed data between groups, while the Chi-square test analyzed categorical variables. Kaplan–Meier (KM) survival analysis evaluated the relationship between disease stage and prognosis. Cox regression models examined independent variables, including clinical factors, FISH, gene mutations, and expression. A partial likelihood test from Cox regression assessed the impact of

these factors on progression-free survival (PFS) and overall survival (OS) in NDMM patients.

Sequencing and bioinformatics analysis

The detailed sequencing steps and bioinformatics analysis methods of WES and RNA-seq can be found in the Supplementary Materials.

Results

Distinct molecular characteristics of NDMM and RRRM

Mutational processes give rise to various combinations of mutation types, known as ‘signatures.’ In the Chinese MM population (cohort 1a & 1b, $n=74$), we identified four distinct mutational signatures that closely resembled signature 1, signature 2, and signature 5 in COSMIC V2 [14] (Fig. 1A). These findings align with the known

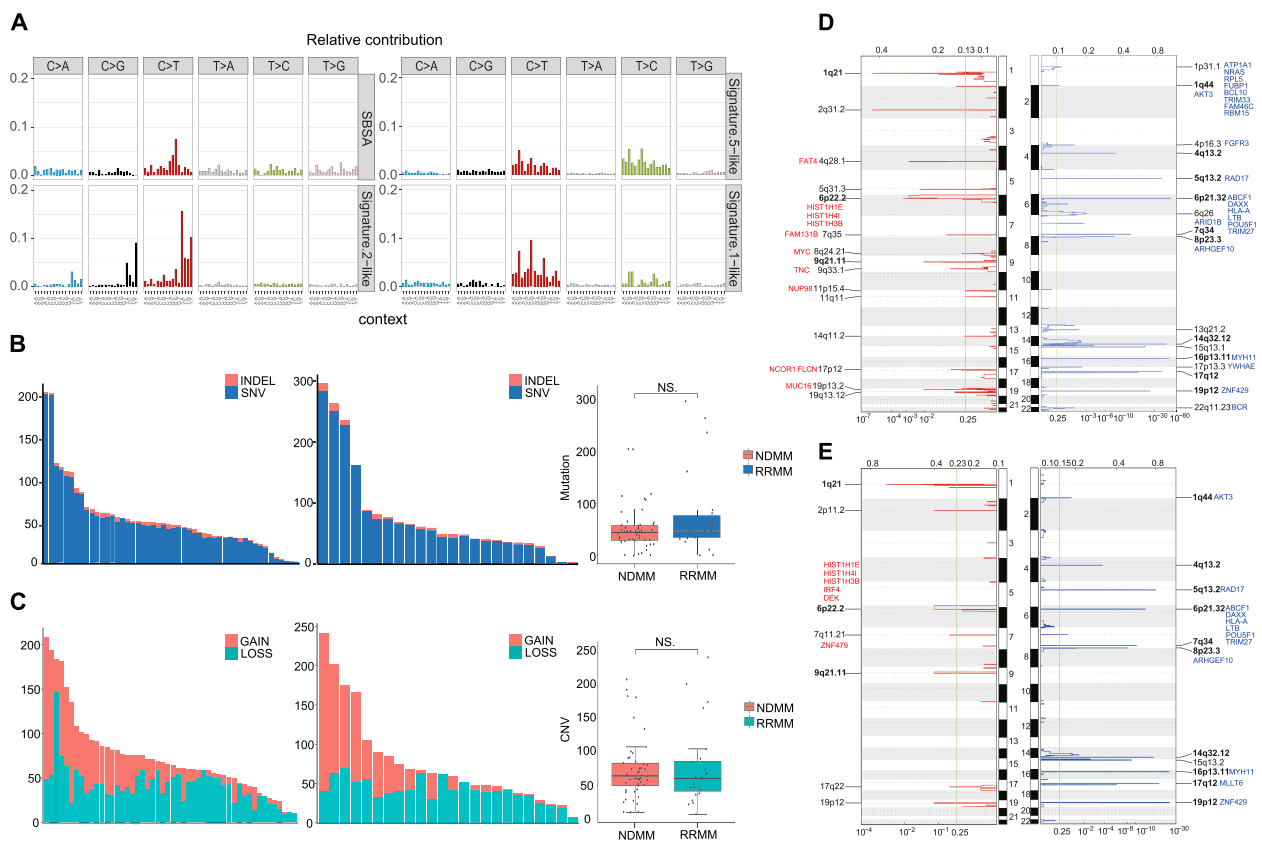


Fig. 1 Distinct molecular characteristics of NDMM and RRRM. **A** Mutational signature identified in Chinese MM patients ($n=74$). A novel signature termed ‘SBSA’ was identified and showed high similarity (cosine similarity=0.78) to signature 15 in COSMIC V2. **B** Comparison of mutation burden between NDMM and RRRM. Each column in the histogram represents a sample, with somatic mutations divided into single nucleotide variant (SNV) and insertion and deletion (INDEL). **C** Comparison of number of segments with CNVs between NDMM and RRRM. Each column in the histogram represents a sample, with CNVs divided into increased copy number (gain) and decreased copy number (loss). **D** The landscape of CNVs of NDMM. Left: Significant ($q < 0.25$) recurrent focal amplified CNVs detected by CNVkit along all autosomes using GISTIC 2.0 are shown. Right: Significant ($q < 0.25$) recurrent focal deleted CNVs detected by CNVkit along all autosomes using GISTIC 2.0 are shown. The Cancer Gene Census (CGC) genes and MM driver genes located in these regions are highlighted and significant CNV regions present in both NDMM and RRRM are displayed in bold font. **E** The landscape of CNVs of RRRM

mutational patterns observed in MM [15]. Moreover, we identified a novel mutational signature, 'SBSA', previously unreported in MM, showing significant similarity (cosine similarity=0.78) to signature 15, associated with defective DNA mismatch repair (dMMR). Supplementary Table 3 details the 96 distinct Single Base Substitution (SBS) patterns from these four signatures and their distribution across samples. We began our investigation into the genomic characteristics of NDMM and RRMM by comparing their mutation burdens. In cohort 1a ($n=50$), the median mutation burden was 1.38 per megabase (IQR=0.86), which was slightly lower than the previously reported value of 1.6 per megabase in MM [16]. The median mutation burden in cohort 1b ($n=24$) increased to 1.45 (IQR=1.26), but this difference was not statistically significant ($p=0.22$, Fig. 1B). Similarly, we compared genomic segments with CNVs between the two groups. In cohort 1a, the median number of segments with increased copy number (gain) was 21 (IQR=35.75), and decreased copy number (loss) was 42.5 (IQR=21.25). In cohort 1b, the medians were 7 (IQR=45.50) and 40 (IQR=17.75) respectively. However, the overall number of CNV segments did not differ significantly between the groups ($p=0.6$, Fig. 1C). Next, we performed somatic CNV analysis using CNVkit [17] and GISTIC 2.0 [18], identifying 15 amplified and 17 deleted recurrent focal CNVs in cohort 1a (Fig. 1D), and 7 amplified and 11 deleted recurrent focal CNVs in cohort 1b (Fig. 1E). These regions were annotated with genes from the Cancer Gene Census (CGC) [19] and 67 MM specific driver genes, as documented in studies by Walker BA et al. (Blood, 2018) [6], Lohr JG et al. (Cancer Cell, 2014) [5], and others [1, 4]. Both groups exhibited common patterns in the recurrent focal CNVs. For example, significantly amplified regions included 1q21, frequently amplified in MM and associated with a poor prognosis [3], 6p22 containing the MM driver gene *HIST1H1E*, and 9q21. The deleted regions showed a higher degree of similarity between the groups, including 6p21, which contains MM driver genes such as *ABCF1*, *HLA-A*, and *LTB*, along with 5q13 harboring the tumor suppressor gene *RAD17*, and 8p23 containing the tumor suppressor gene *ARHGEF10*, among others. Additionally, cohort 1b displayed unique

significant amplifications in regions such as 2p11, 7q11, 17q22, and 19p12, distinguishing it from cohort 1a. To delineate the transcriptional differences between NDMM and RRMM patients, we conducted a comparative analysis of differential gene expression and associated pathways. Our analysis revealed significant upregulation of pathways involved in 'nucleosome assembly,' 'axon guidance,' and 'cell recognition' in the RRMM cohort ($n=41$) compared to the NDMM cohort ($n=84$), implying an enhanced capacity for tumor proliferation and chemoresistance in RRMM. In contrast, the downregulation of 'T cell activation,' 'forebrain development,' and 'gland development' pathways in RRMM may point to a diminished immune response and tumor dedifferentiation, key factors in disease recurrence and resistance to therapy (Supplementary Figure 2). These insights into the pathogenesis of RRMM could inform the development of novel therapeutic strategies.

Recurrent mutated genes in NDMM and RRMM

In addition to the differences in overall molecular characteristics, we aim to investigate how highly mutated genes differ between NDMM and RRMM patients.

In cohort 1a, we identified 48 genes that were recurrently mutated above a 5% threshold, accounting for 82% of the total samples (Fig. 2A). Notably, among these genes were *KRAS*, *NRAS*, *DIS3*, *HIST1H1E*, *NFKBIA*, *ZNF292*, and *DUSP2*, which are recognized as driver genes in MM [1, 4–6], with *KRAS* and *NRAS* confirmed by MutSigCV [20]. We analyzed the frequency of these seven driver genes in cohort 1a ($n=50$) compared to the MMRF-COMMPASS cohort ($n=937$), as presented in Supplementary Table 4. Interestingly, the mutation frequency of *NFKBIA* in cohort 1a was significantly elevated (4/50 vs 22/937, $p=0.048$, Fig. 2B). Specifically, *NFKBIA* mutations were identified in 4 patients within cohort 1a, including 2 frame-shift deletions and 1 nonsense mutation, all of which may affect the gene's function, indicating a potential role in disease pathology (Fig. 2C). These mutation sites were manually confirmed using Integrative Genomics Viewer (IGV) (Supplementary Figure 3). A comparison of *NFKBIA* gene expression between

(See figure on next page.)

Fig. 2 Recurrent mutated genes in NDMM. **A** Waterfall of NDMM patients' gene mutations. All genes are divided into three groups, genes identified as SMGs by MutsigCV (SMG), previously reported SMGs (Public SMG) and some novel mutant genes (Novel). In the third group, six genes also appear in the validation cohort (cohort 1A, $n=77$) at a higher frequency ($>5\%$) are marked with an asterisk. Related clinical characteristics of all patients are shown at the top, including sex, age at diagnosis, DS stage, ISS stage, R-ISS stage and sum of FISH results, which include t(4;14), t(14;16) and 17p-. DS Durie-Salmon, ISS International Staging System, R-ISS Revised International Staging System, FISH fluorescence in situ hybridization, SMG significantly mutated gene. **B** Frequency comparison of SMGs between cohort 1a and MMRF-COMMPASS. **C** *NFKBIA* somatic mutation sites in cohort 1a

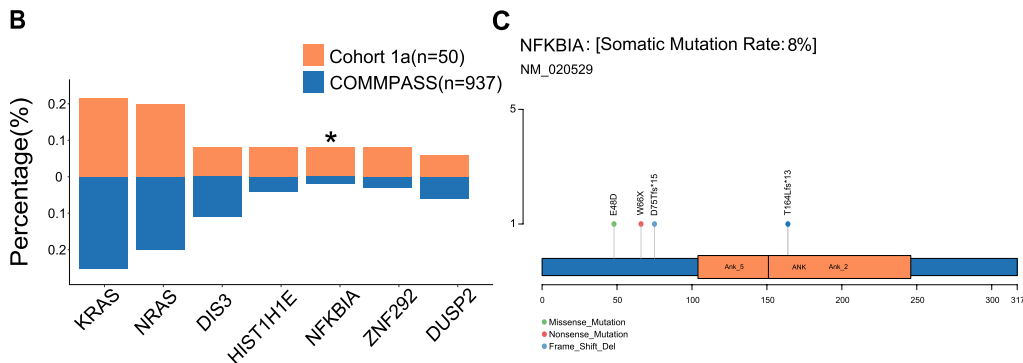
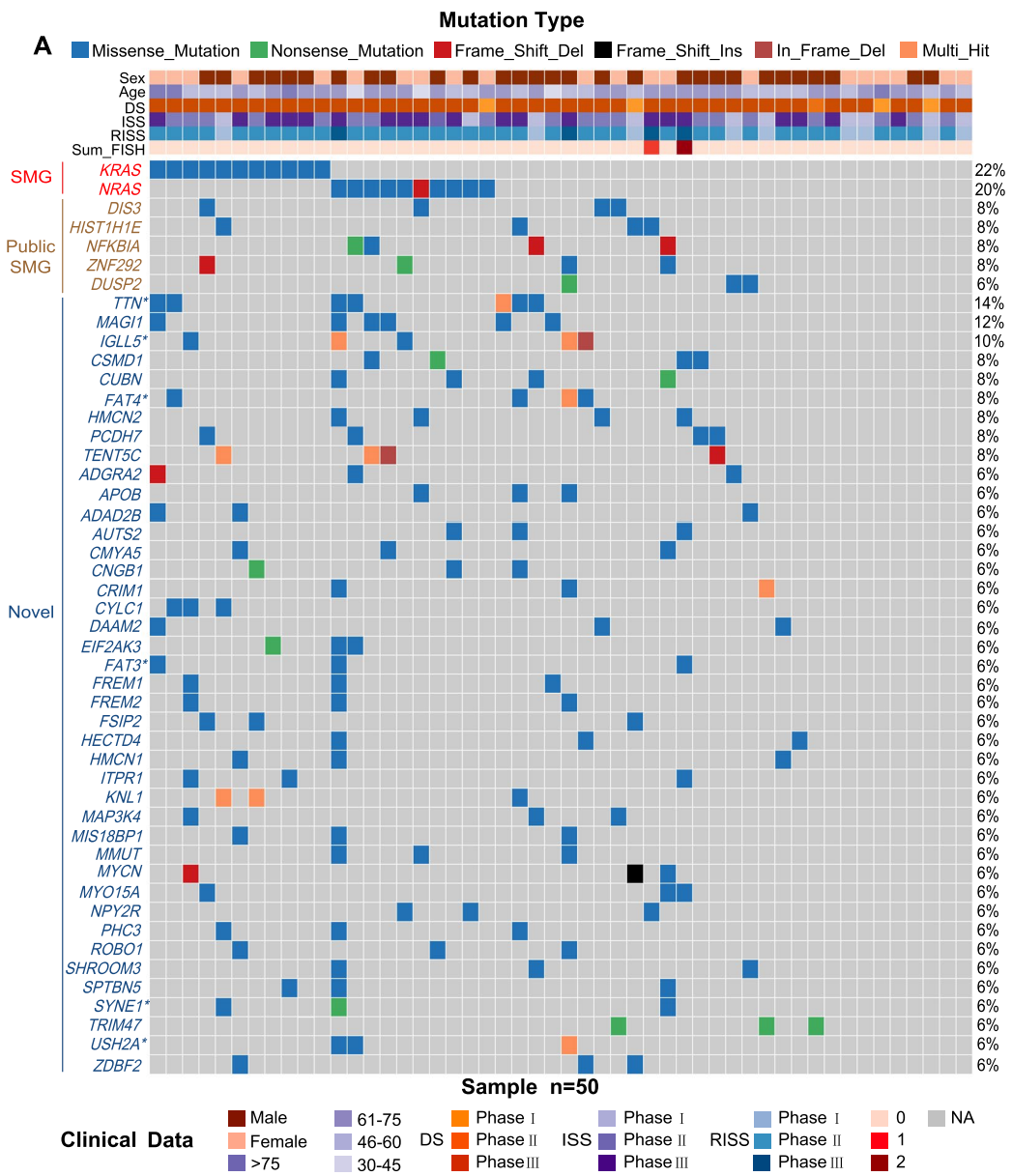


Fig. 2 (See legend on previous page.)

mutated and non-mutated samples showed no significant difference in expression levels after excluding CNV interference (Supplementary Figure 4A). Alongside the seven previously identified driver genes, we also identified 41 genes with recurrent mutations in cohort 1a, including *TTN*, *FAT4*, *FAT3*, and *IGLL5*. To validate these findings, we analyzed cohort 1A ($n=77$), specifically excluding mutation sites with variant allele frequencies (VAF) near 50% and 100% to minimize the inclusion of germline mutations. We confirmed the presence of 27 out of these 41 genes in cohort 1A. Notably, six genes—*TTN*, *FAT4*, *FAT3*, *SYNE1*, *USH2A*, and *IGLL5*—exhibited mutation frequencies greater than 5% (Supplementary Figure 4B). The specific locations of these mutations are detailed in Supplementary Figure 4C.

Similarly, we identified 22 genes in cohort 1b with mutation frequencies greater than 10%, which accounts for 75% of the cohort (Fig. 3A). Of these, seven genes were previously identified as driver genes in MM [1, 4–6], with *KRAS* recognized as a driver gene by MutSigCV [20]. We compared the mutation frequencies of these seven driver genes between cohorts 1a and 1b. Notably, *UBR5* exhibited a higher mutation frequency in cohort 1b, showing a statistically significant difference (4/24 vs 0/50, $p=0.01$, Fig. 3B). In cohort 1b, *UBR5* contained four mutation sites, all of which were confirmed by IGV (Supplementary Figure 5). The W2715X and C2768W mutations were located within the homology to E6-AP carboxyl terminus (HECT) domain of *UBR5*, while T689I and L1519R were outside this domain (Fig. 3C). A further comparison of *UBR5* gene expression between mutated and non-mutated samples indicated that W2715X expression was slightly lower when CNV interference was excluded (Supplementary Figure 6A). In addition to the seven driver genes, we also identified 15 recurrently mutated genes in cohort 1b. Among these, nine genes were confirmed in cohort 1B ($n=37$), with five exhibiting mutation frequencies above 5%, including *OBSCN*, *HSPG2*, *CACNA1H*, *IGLL5*, and *PCLO* (Supplementary Figures 6B, 6C).

Clonal evolution in MM

To investigate the temporal and spatial heterogeneity of MM, we established several research cohorts through multi-time and multi-site sampling of individual patients. From a spatial perspective, prior studies have demonstrated that CPCs are derived from BM-PCs and are typically associated with a poor prognosis [21, 22]. Our study not only corroborates these findings but also identifies several genes that potentially involved in the development of CPCs. In patients 189 and 190, we observed shared mutations between BM-PCs and CPCs, including *CSMD3*, *GOLGA5*, and *TGDS* in patient 189, as well as

RBM15, *NCKIPSD*, and *LIFR* in patient 190, suggesting a common progenitor for these cells. During the transition from BM-PCs to CPCs, we observed a dynamic clonal shift. Specifically, clones harboring *CSF1R* and *TRAF3* gradually diminished in patient 189, while a novel clone containing *SNX29*, *OLIG2*, and *BMPRIA* emerged (Fig. 4A). A similar pattern was observed in patient 190, characterized by the disappearance of clones containing *FAM135B* and *CIITA*, alongside the emergence of a new clone containing *LRP1B* (Fig. 4B). These findings underscore a pattern of clonal evolution during the differentiation of CPCs, characterized by shared mutations and the selective disappearance and emergence of specific clones.

From a temporal perspective, as the disease state evolves, the clonal populations of tumor cells within the patient also undergo corresponding changes. In patient 193, there was a gap of 334 days between the initial diagnostic sampling and subsequent resampling conducted at the point of disease progression. The FISH analyses of both samples revealed no significant differences; however, a notable variation was observed in the genetic mutations (Fig. 4C). Mutations in genes such as *NRAS*, *FAT4*, *RGS7*, *MNI*, and *MET* were observed in both samples over time, suggesting that the administered treatment regimen may not effectively target these clones. Importantly, the frequency of specific mutations shifted, with subclones harboring mutations in *OBSCN* and *CACNA1H* displaying a gradual increase. These two genes have been identified as novel recurrently mutated genes in RRMM samples (Fig. 3A), highlighting their potentially significant role in disease progression. Furthermore, as the disease progressed, a distinct subclone emerged, possessing mutations in *CDKN2C* and *KNL1*. In patient 209, a similar pattern of clonal evolution from remission to progression phases was observed (Fig. 4D). Notably, during the progression phase, there was a significant increase in the proportion of clones harboring *TP53* mutations, underscoring the critical significance of this gene in the disease. Beyond the previously mentioned four patients, we documented the gene mutations alterations across multi time points or site in 20 additional patients. Notably, patients 211 and 212 exhibited clonal evolution throughout the disease course, suggesting that this phenomenon is common among MM patients (Supplementary Figure 7).

Prognosis analysis

We performed a comprehensive analysis to evaluate the impact of mutation status and expression levels of key genes, recognized as MM driver genes or newly identified as recurrently mutated genes (indicated by "SMG", "Public SMG", or asterisk in Figs. 2A and 3A) on the prognosis of NDMM patients. This analysis included 58

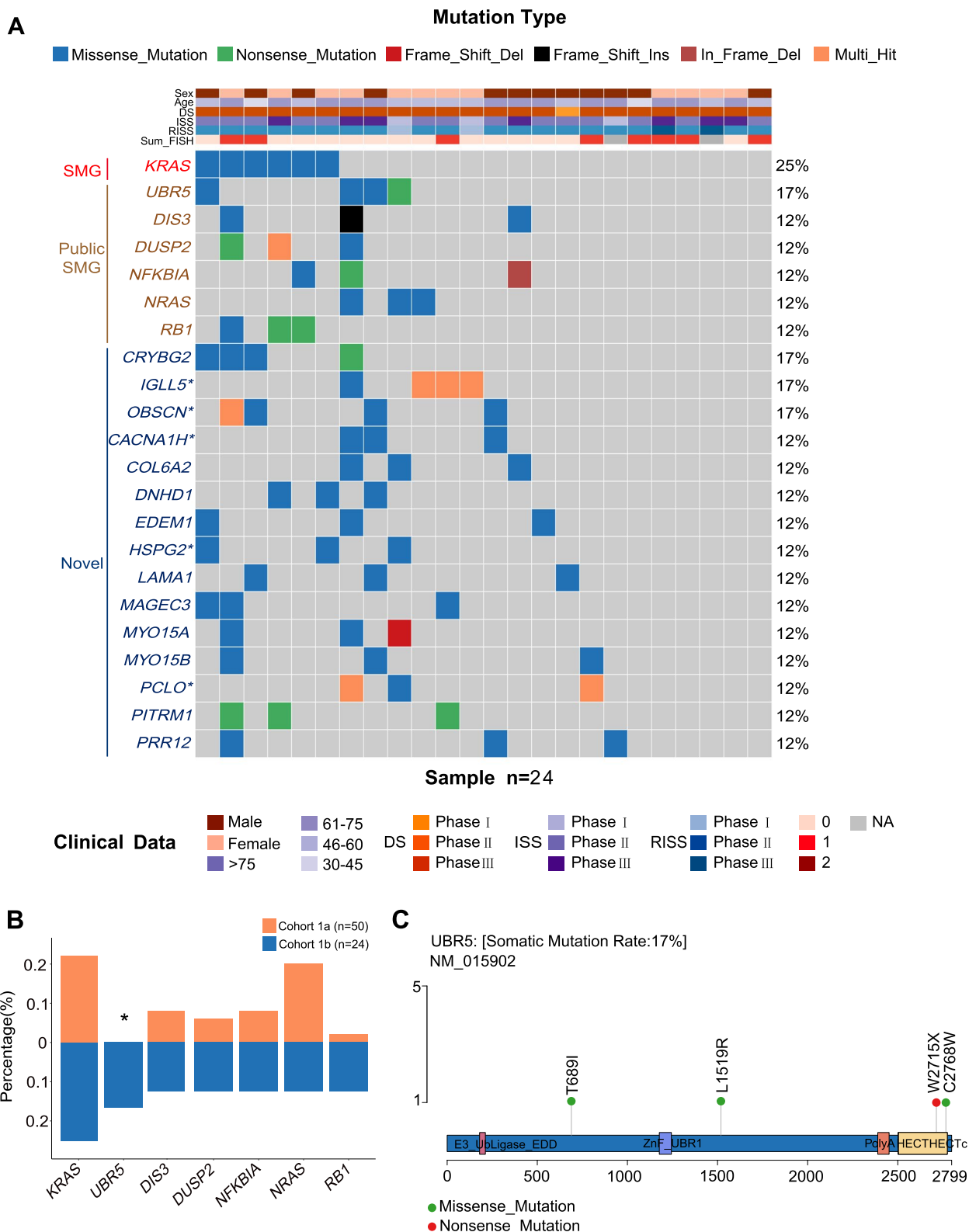


Fig. 3 Recurrent mutated genes in RRRM. **A** Waterfall of RRRM patients' gene mutations. **B** Frequency comparison of SMGs between cohort 1a and cohort 1b. **C** *UBR5* somatic mutation sites in cohort 1b

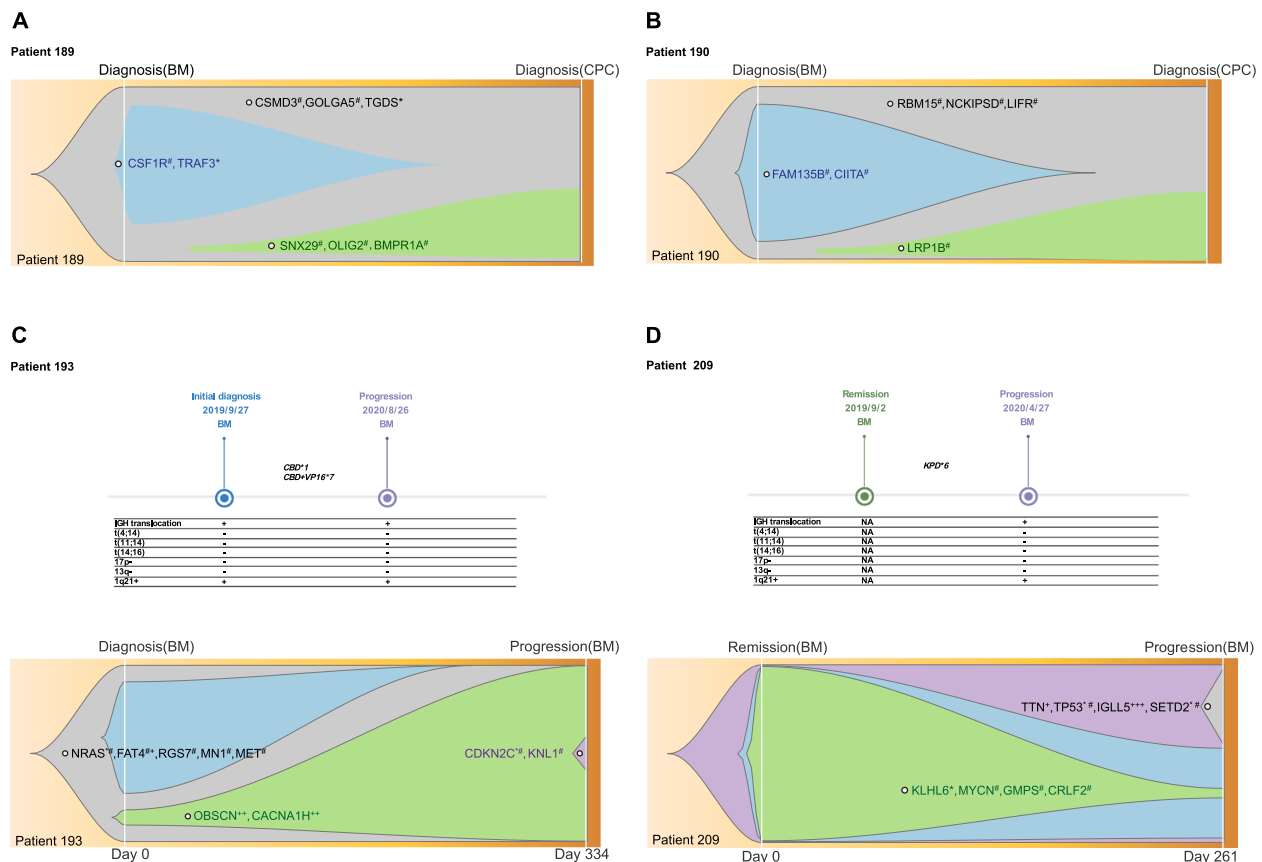


Fig. 4 Clonal evolution in MM. **A** Clonal evolution of patient 189. Fishplot showing dynamic clonal evolution from BM-PCs to CPCs in patient 189. **B** Clonal evolution of patient 190. Fishplot showing dynamic clonal evolution from BM-PCs to CPCs in patient 190. **C** Clonal evolution of patient 193. Fishplot showing dynamic clonal evolution of patient 193 when disease progressed from the initial diagnosis. **D** Clonal evolution of patient 209. Fishplot showing dynamic clonal evolution of patient 209 when disease progressed from the remission phase. ^{***} SMGs, [#] Cancer Gene Census (CGC) genes, ⁺⁺ novel recurrent mutated genes identified in NDMM patients, ⁺⁺⁺ novel recurrent mutated genes identified in RRMM patients, CBD C: cyclophosphamide; B: bortezomib; D: dexamethasone, VP16 etoposide, KPD K: carfilzomib; P: pomalidomide; D: dexamethasone, + positive, — negative, NA not available

parameters, such as clinical factors (e.g., sex, age, and hemoglobin levels), FISH, and the mutation and expression profiles of key genes. We evaluated the prognostic influence in 64 NDMM patients using both univariate and multivariate Cox regression analyses (Supplementary Table 5). Initially, patients were stratified according to the International Staging System (ISS) and the Revised-ISS (R-ISS). Patients classified as phase III by ISS and R-ISS exhibited poorer prognoses, reinforcing the reliability of our prognostic data (Supplementary Figure 8).

In the analysis of PFS, univariate analysis identified six significant predictors (Fig. 5A). Specifically, age (ref.Low, HR=1.04 [95% CI, 1.01 to 1.08], $p=0.016$), $\beta 2$ microglobulin ($\beta 2$ -MG) (ref.Low, HR=1.03 [95% CI, 1.01 to 1.05], $p=0.014$), and ISS phase III (ref.Other, HR=2.99 [95% CI, 1.19 to 7.54], $p=0.02$) were associated with adverse outcomes. Moreover, mutations in *OBSCN* (ref.Negative, HR=5.80 [95% CI, 1.68 to 20.06],

$p=0.005$) and *RBI* (ref.Negative, HR=31.00 [95% CI, 2.81 to 341.85], $p=0.005$) had a significant negative impact on PFS. Although *IGLL5* expression (ref.Low, HR=1.00 [95% CI, 1.00 to 1.00], $p=0.021$) was statistically significant, it did not have a substantial effect on PFS. The multivariate analysis further confirmed the negative impacts of age (ref.Low, HR=1.04 [95% CI, 1.00 to 1.08], $p=0.04$), *OBSCN* mutations (ref.Negative, HR=5.11 [95% CI, 1.31 to 19.95], $p=0.019$), and *RBI* mutations (ref.Negative, HR=83.56 [95% CI, 5.75 to 1213.75], $p=0.001$) on PFS. The expression of *IGLL5* continued to show no significant effect on PFS (ref.Low, HR=1.00 [95% CI, 1.00 to 1.00], $p=0.001$) (Fig. 5B). In the analysis of OS, univariate analysis identified five significant prognostic factors (Fig. 5C). Hemoglobin (Hb) (ref.Low, HR=0.96 [95% CI, 0.93 to 1.00], $p=0.033$) and serum albumin (ALB) (ref.Low, HR=0.89 [95% CI, 0.81 to 0.99], $p=0.024$) positively influenced OS.

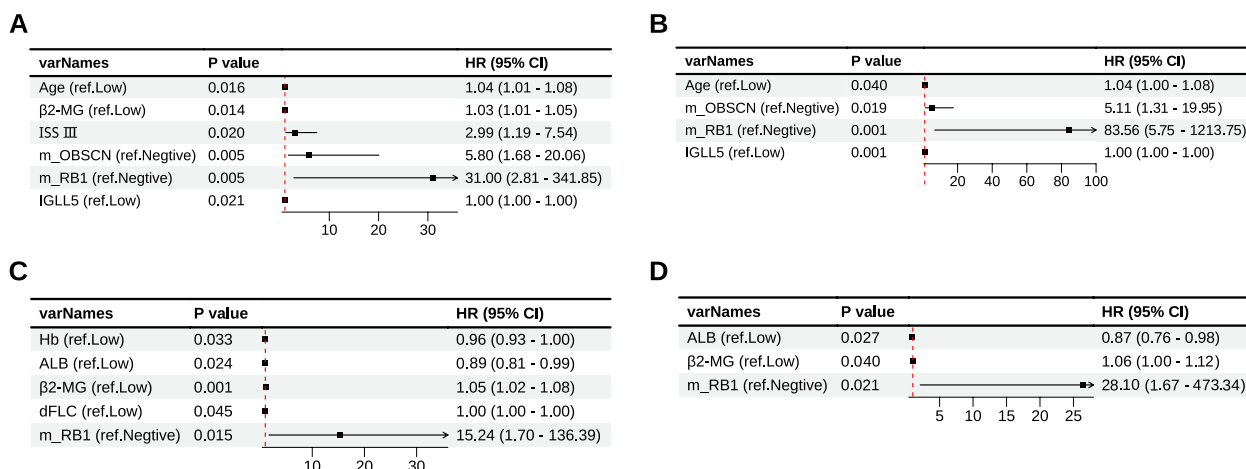


Fig. 5 Prognosis analysis of 64 NDMM patients. **A** Univariate cox logistic regression analysis of PFS in 64 NDMM patients. **B** Multivariate cox logistic regression analysis of PFS in 64 NDMM patients. **C** Univariate cox logistic regression analysis of OS in 64 NDMM patients. **D** Multivariate cox logistic regression analysis of OS in 64 NDMM patients. m_OBSCN mutation of *OBSCN*, m_RB1 mutation of *RB1*, IGLL5 expression of *IGLL5*, Hb hemoglobin, ALB serum albumin, dFLC difference between involved and uninvolved free light chain

Conversely, β 2-MG (ref.Low, HR=1.05 [95% CI, 1.02 to 1.08], $p=0.001$) and *RB1* mutations (ref.Negative, HR=15.24 [95% CI, 1.70 to 136.39], $p=0.015$) were associated with unfavorable impacts on OS. Although the differential between involved and uninvolved free light chains (dFLC) was statistically significant, it showed no significant influence on OS (reference: Low, HR=1.00 [95% CI, 1.00 to 1.00], $p=0.045$). Multivariate analysis confirmed the significance of ALB, β 2-MG, and *RB1* mutations (Fig. 5D). ALB positively influenced OS (ref.Low, HR=0.87 [95% CI, 0.76 to 0.98], $p=0.027$), while β 2-MG (ref.Low, HR=1.06 [95% CI, 1.00 to 1.12], $p=0.04$) and *RB1* mutations (ref.Negative, HR=28.10 [95% CI, 1.67 to 473.34], $p=0.021$) were associated with adverse effects.

Discussion

This study presents several novel discoveries, primarily the identification of a new mutational signature in Chinese NDMM patients. A mutational signature is widely recognized as a unique combination of mutations resulting from specific etiological factors. Investigating these signatures is essential for identifying the underlying causes and mechanisms of diseases, thereby improving our understanding and encouraging further scientific research. Here, we identified a novel mutational signature, referred to as 'SBSA', associated with dMMR which plays a vital role in detecting and correcting genetic discrepancies. A malfunction in this biomarker results in an accumulation of mutations and the formation of neoantigens that trigger an immune response against tumors [23]. Previous clinical trials have shown that dMMR is

associated with improved responses and favorable prognoses in specific cancers treated with immune checkpoint inhibitors (ICIs) [24–26]. The application of ICIs in MM is currently being investigated. Previous research has indicated that the use of PD-1 and PD-L1 monoclonal antibodies including pembrolizumab and nivolumab as monotherapy for MM has not demonstrated significant therapeutic benefits. Yet, when these antibodies are integrated with other treatment modalities, including immunomodulators, proteasome inhibitors, and CAR-T cell therapies, they can achieve notable therapeutic outcomes. This finding implies that the use of PD-1 and PD-L1 monoclonal antibodies in the treatment of MM retains considerable potential for clinical application [27–30].

Furthermore, our study reveals significant disparities between Asian and Western NDMM patients. In our comparative analysis involving the publicly available MMRF-COMMPASS cohort ($n=973$), we observed a higher prevalence of *NFKBIA* mutations among Chinese NDMM patients ($n=50$). The *NFKBIA* gene encodes the protein NF- κ B inhibitor α ($I\kappa$ B α), which plays a crucial role in regulating cellular immune responses, inflammatory reactions, and cell survival. *NFKBIA* functions by inhibiting the activity of the NF- κ B transcription factor. In its inactive state, the NF- κ B transcription factor is bound to $I\kappa$ B α . Upon cellular stimulation, $I\kappa$ B α undergoes degradation, which releases NF- κ B, allowing it to enter the nucleus and activate the expression of various genes. In cancer research, *NFKBIA*'s function is particularly significant as abnormal activation of the NF- κ B pathway is closely associated with the development of

various cancers. For instance, mutations or dysregulation of *NFKBIA* can result in persistent activation of NF- κ B, thereby promoting tumor cell survival and proliferation, and resistance to apoptosis. Studies indicate that in certain types of cancer, including breast cancer, ovarian cancer, and Hodgkin lymphoma, abnormal expression of *NFKBIA* is related to disease prognosis and treatment response [31–34]. In this study, we observed a significantly increased mutation frequency of *NFKBIA* in Chinese NDMM patients, with the mutations predominantly being frameshift deletions and nonsense mutations. This finding implies that *NFKBIA* may activate the NF- κ B pathway via alterations in its function, contributing to the pathogenesis and progression of MM. Currently, a variety of inhibitors targeting complexes and biological processes within the NF- κ B pathway, such as the IKK complex, I κ B, and p65 acetylation, have been developed and are being used in cancer treatment [35, 36]. Our study has identified a marked increase in the mutation frequency of the *NFKBIA* gene, encoding the I κ B α protein, in Chinese NDMM patients. This finding implicates the potential therapeutic utility of NF- κ B pathway inhibitors in this patient group. Meanwhile, studies have shown that in cervical cancer, activation of the NF- κ B pathway can increase the expression of PD-L1, leading to tumor progression [37]. The use of ICIs has shown promising therapeutic effects, which further underscores the potential merit of investigating the use of ICIs in MM.

Moreover, we have identified significant differences between NDMM and RRMM patients. In RRMM patients, a high frequency of *UBR5* mutations was observed. *UBR5* encodes a protein that is induced by progestin and belongs to the HECT family. Members of this family act as E3 ubiquitin-protein ligases, targeting specific proteins for ubiquitin-mediated proteolysis [38]. *UBR5* plays a crucial role in hematological malignancies. Approximately 18% of patients with mantle cell lymphoma (MCL) exhibit *UBR5* mutations, primarily located within its HECT domain which is responsible for accepting and transferring ubiquitin molecules to substrates. The loss of the *UBR5* HECT domain inhibits B-cell maturation in the spleen and results in the upregulation of proteins involved in mRNA splicing via the spliceosome, which is vital for the transformation in MCL [39]. In our study, we identified four mutation sites in *UBR5*: two (W2715X and C2768W) within the HECT domain and two (T689I and L1519R) outside of it. In clinical practice, proteasome inhibitors are widely used as a primary treatment modality for MM. They function by inhibiting proteasome subunits and reducing the degradation of misfolded proteins within MM cells, thereby inducing endoplasmic reticulum stress and promoting cell death [40]. The elevated mutation frequency of *UBR5* in RRMM

patients suggests that these mutations may enable MM cells to enhance the activity of E3 ubiquitin-protein ligases. This enhancement could promote the degradation of misfolded intracellular proteins or facilitate drug resistance and disease progression through alternative pathways. Additional experiments are needed to validate these hypotheses. Additionally, we have identified several frequently mutated genes in NDMM and RRMM patients, including *TTN*, *IGLL5*, *FAT4*, *FAT3*, *SYNE1*, *USH2A*, *CACNA1H*, *OBSCN*, *HSPG2*, and *PCLO*. Certain genes, such as *TTN* and *FAT4*, exhibit a higher mutation frequency, which is partially attributable to their extended length and recent studies have indicated that these genes may play significant roles in tumors as well [41–43]. Meanwhile, genes such as *IGLL5* have been shown to be closely associated with B-cell lymphoma [44, 45]. Therefore, we believe that these newly identified frequently mutated genes could serve as promising targets in the study of MM, enhancing our understanding of disease initiation and progression.

Our study has additionally uncovered clonal evolution in MM from both temporal and spatial perspectives through sampling at various time points and locations. Spatially, we concentrate on the relationship between CPCs and BM-PCs. Previous studies have characterized CPCs derived from MM patients from various aspects including cytogenetics, gene expression profiles, and gene mutations [21, 46, 47]. On one hand, CPCs exhibit genomic features similar to BM-PCs, such as chromosomal abnormalities and gene mutations including chromosomal translocations, amplifications, deletions, and mutations in genes like *KRAS*, *NRAS*, *TP53*, and *MYC*. On the other hand, CPCs display unique molecular biological changes, such as a notably increased proportion of the t(11;14) translocation often accompanied by high expression of the *CCND1* gene, and their DNA methylation and histone modification patterns are significantly different from those of BM-PCs. Our findings indicate that CPCs likely originate from BM-PCs due to their shared ancestral mutations. During the process of evolution, there is often the disappearance of old clones and the emergence of new clones. Genes such as *SNX29*, *OLIG2*, *BMRP1A*, and *LRP1B* may be associated with the formation of CPCs. Temporally, clonal evolution occurs at various stages of the disease, including initial diagnosis, disease progression, and remission. For instance, during disease progression, mutations in specific genes, such as *OBSCN*, *CACNA1H*, and *TP53*, frequently arise, indicating a strong correlation between these genes and disease progression. Additionally, we observed that in some patients, FISH results do not exhibit significant changes between initial diagnosis and disease progression. However, in reality, there has been substantial clonal evolution

of tumor cells within the patient's body. This finding suggests that NGS may offer greater precision than FISH technology in monitoring the disease.

In our comprehensive analysis using extensive WES and RNA-seq datasets, we identified several prognostic biomarkers for NDMM patients. These biomarkers have the potential to predict outcomes and guide therapeutic strategies for MM patients. Specifically, we found that advanced age and mutations in *OBSCN* and *RBI* significantly increase the risk of disease progression in NDMM patients regarding PFS. In terms of OS, elevated levels of ALB act as a protective factor, while high β 2-MG levels pose a risk, consistent with the ISS criteria [48, 49]. Furthermore, mutations in the *RBI* gene significantly increase the mortality risk of NDMM patients. Among these two biomarkers, *OBSCN* encodes giant obscurins (720–870 kDa), initially identified in striated muscles as cytoskeletal proteins with scaffolding and regulatory functions. Recently, it has emerged as a crucial factor in cancer biology. Research indicates that *OBSCN* plays a significant role in various cancers, including those of the brain, gastrointestinal tract, kidneys, female reproductive system, and pancreas [50, 51]. For example, in triple-negative breast cancer, restoration of *OBSCN* via *OBSCN*-AS1 long-noncoding RNA CRISPR-targeting curtails metastasis and influences cell migration through RhoA-dependent cytoskeletal remodeling [52]. Typically, *OBSCN* primarily functions as a tumor suppressor gene. Our findings indicate that mutations in *OBSCN* are associated with shorter remission durations in NDMM patients. This highlights its prognostic significance and call for further research into its underlying molecular mechanisms. Another gene of prognostic importance is *RBI*, the first tumor suppressor gene to be molecularly characterized, with mutations observed in a wide range of malignancies including prostate, lung, and breast cancers, as well as virtually all cases of familial and sporadic retinoblastoma [53, 54]. Our study indicates that NDMM patients with *RBI* mutations experience significantly reduced PFS and OS, highlighting *RBI*'s critical role in MM. Whether *RBI* functions similarly as a tumor suppressor in other cancers remains an area for further confirmation. These biomarkers present valuable insights for risk stratification and personalized medicine, potentially leading to more precise and effective interventions in the management of MM.

The current study acknowledges several limitations. First, the study cohort was relatively small, necessitating validation of prognostic biomarkers such as *RBI* and *OBSCN* mutations in larger cohorts. Second, the study primarily focuses on sequencing analysis, lacking comprehensive functional validation. Future research should

integrate functional assays or experimental models to confirm these discoveries' implications. Despite these constraints, the sequencing data derived from this study provide valuable insights into the genomic landscape of the condition under investigation. The identified mutations and prognostic biomarkers can serve as a starting point for further research, guiding future studies and investigations into the underlying mechanisms involved.

Conclusions

Through the application of WES and RNA-seq, we have uncovered several pivotal insights. Firstly, we identified a novel mutational signature in Chinese MM patients, implicating the potential involvement of the dMMR mechanism in the pathogenesis of MM. Secondly, through a comparative analysis of Chinese and Western cohorts, we observed that the mutation frequency of *NFKBIA* is significantly higher in Chinese NDMM patients, whereas the mutation frequency of *UBR5* is elevated in RRMM patients. Thirdly, by conducting multi-site sampling in MM patients, we substantiated the occurrence of clonal evolution in MM both temporally and spatially, and identified genes that may play critical roles in this process. Lastly, through prognostic analysis integrating clinical indicators and genetic characteristics, we validated the prognostic significance of age, β 2-microglobulin, and albumin in MM. Additionally, for the first time, we demonstrated that mutations in *OBSCN* and *RBI* significantly impact the prognosis of NDMM patients.

Abbreviations

BM	Bone marrow
CPC	Circulating plasma cell
CNVs	Copy number variations
dMMR	Defective DNA mismatch repair
FISH	Fluorescence in situ hybridization
HRD	Hyperdiploid
HECT	Homology to E6-AP carboxyl terminus
ISS	International Staging System
ICIs	Immune checkpoint inhibitors
MM	Multiple myeloma
MGUS	Monoclonal gammopathy of undetermined significance
NGS	Next-generation sequencing
NDMM	Newly diagnosed MM
OS	Overall survival
PFS	Progression-free survival
RRMM	Relapsed/refractory MM
RNA-seq	RNA sequencing
SMM	Smoldering MM
SMG	Significantly mutated genes
WES	Whole-exome sequencing

Supplementary Information

The online version contains supplementary material available at <https://doi.org/10.1186/s12920-025-02116-5>.

Supplementary Material 1: Supplementary Figure 1. Schematic diagram of research cohorts. The left part shows the cohort of WES samples. 212

Chinese MM patients were sampled by different methods, and 242 tumor samples were obtained and sequenced by WES. Whereas 'Matched' indicates that tumor samples are accompanied by normal peripheral blood samples from the same patient as controls, 'Unmatched' signifies that only tumor samples from the patient are obtained. Among them, 131 tumor samples were sequenced by RNA-seq at the same time, and these samples are shown on the right side. The two digits separated by slashes in each cell represent the total number of patients and the corresponding total number of tumor samples, respectively.

Supplementary Material 2: Supplementary Figure 2. Transcriptomic differences between NDMM and RRMM. A Volcano plot of the RNA-seq data of RRMM ($n=41$) versus NDMM patients ($n=84$). Significantly upregulated (red) and downregulated (blue) genes are highlighted ($|\log_2FC| > 1$, P value < 0.01). Significant differential expressed genes and newly identified as recurrently mutated genes in NDMM and RRMM like *TTN* and *USH2A*, were labeled. B GO analysis of significantly dysregulated genes in RRMM and NDMM patients. The pathways depicted above are upregulated, while those below are downregulated. Biological processes were selected based on the count of gene number (gene count > 10) and P value (< 0.01).

Supplementary Material 3: Supplementary Figure 3. Manually check of *NFKBIA*'s mutation sites by IGV.

Supplementary Material 4: Supplementary Figure 4. Expression of *NFKBIA* and 41 recurrent mutated genes' frequencies in cohort 1A. A Comparison of gene expression between *NFKBIA* mutant and wild type. B Frequencies of 41 recurrent mutated genes in cohort 1A. Using 5% as the frequency dividing line, six genes with high mutation rates including *TTN*, *FAT4*, *FAT3*, *SYNE1*, *USH2A* and *IGLL5* were screened. C Lollipop plots of these six genes' somatic mutation sites in cohort 1a.

Supplementary Material 5: Supplementary Figure 5. Manually check of *UBR5*'s mutation sites by IGV.

Supplementary Material 6: Supplementary Figure 6 Expression of *UBR5* and 15 recurrent mutated genes' frequencies in cohort 1B. A Comparison of gene expression between *UBR5* mutant and wild type. B Frequency of 15 recurrent mutated genes in cohort 1B. Using 5% as the frequency dividing line, five genes with high mutation rates including *OBSN*, *HSPG2*, *CACNA1H*, *IGLL5* and *PCLO* were screened. C Lollipop plots of these five genes' somatic mutation sites in cohort 1b.

Supplementary Material 7: Supplementary Figure 7. Treatment process and mutation changes of 20 MM patients. We described the treatment process and mutation changes of 20 MM patients and the fishplot illustrates the spatio-temporal dynamics of clonal evolution in patients 211 and 212. BM bone marrow, CPC circulating plasma cell, + positive, - negative, NA not accessible,*** SMGs,*** Cancer Gene Census (CGC) genes, "+" novel recurrent mutated genes identified in NDMM patients, "+" novel recurrent mutated genes identified in RRMM patients, V(T)(R)(C)(P) D V: bortezomib; T: thalidomide; R: lenalidomide; C: cyclophosphamide; P: pomalidomide; D: dexamethasone, CB(R)D C: cyclophosphamide; B: bortezomib; R: lenalidomide; D: dexamethasone, VP16 etoposide, Bi-VRDAEP Bi: clarithromycin; VRD; A: adriamycin; E: etoposide; P: platin, Bi-RD Bi: clarithromycin, RD, IRD I: ixazomib, RD, D(R)(V)(T)D D: daratumumab; R: lenalidomide; V: bortezomib; T: thalidomide; D: dexamethasone, Auto-HSCT autologous hemopoietic stem cell transplantation, CAR-T chimeric antigen receptor T cell.

Supplementary Material 8: Supplementary Figure 8. Kaplan-Meier (KM) survival analysis of 64 NDMM patients. ISS International Staging System, R-ISS Revised International Staging System.

Supplementary Material 9.

Supplementary Material 10.

Supplementary Material 11.

Supplementary Material 12.

Supplementary Material 13.

Supplementary Material 14.

Acknowledgements

Not applicable.

Authors' contributions

XC, JL and JD designed the study, wrote the main manuscript text and prepared figures. XC, TCL, WHZ and SW performed data curation, formal analysis and visualization. MXZ, XNZ and SZ provided software support. HYH, JL, JL, WTQ, YCJ and NH performed data curation and formal analysis.

Funding

This work was supported by National Natural Science Foundation of China (NSFC) [grant numbers 82170198, 81070164, 81372543].

Data availability

The raw sequence data reported in this paper have been deposited in the Genome Sequence Archive (Genomics, Proteomics & Bioinformatics 2021) in National Genomics Data Center (Nucleic Acids Res 2022), China National Center for Bioinformation / Beijing Institute of Genomics, Chinese Academy of Sciences (GSA-Human: HRA005897) that are publicly accessible at <https://ngdc.cncb.ac.cn/gsa-human>.

Declarations

Ethics approval and consent to participate

This study was approved by the Ethics Committee of Shanghai Changzheng Hospital (2016SL019A) and conducted in accordance with the the World Medical Association Declaration of Helsinki. An informed consent protocol was used for this study and written informed consent was obtained from all the patients.

Consent for publication

Not applicable.

Competing interests

The authors declare no competing interests.

Received: 27 October 2024 Accepted: 27 February 2025

Published online: 14 March 2025

References

- Chapman MA, Lawrence MS, Keats JJ, Cibulskis K, Sougnez C, Schinzel AC, et al. Initial genome sequencing and analysis of multiple myeloma. *Nature*. 2011;471(7339):467–72.
- Walker BA, Boyle EM, Wardell CP, Murison A, Begum DB, Dahir NM, et al. Mutational spectrum, copy number changes, and outcome: results of a sequencing study of patients with newly diagnosed myeloma. *J Clin Oncol*. 2015;33(33):3911–20.
- Walker BA, Leone PE, Chiecchio L, Dickens NJ, Jenner MW, Boyd KD, et al. A compendium of myeloma-associated chromosomal copy number abnormalities and their prognostic value. *Blood*. 2010;116(15):e56–65.
- Bolli N, Avet-Loiseau H, Wedge DC, Van Loo P, Alexandrov LB, Martincorena I, et al. Heterogeneity of genomic evolution and mutational profiles in multiple myeloma. *Nat Commun*. 2014;5:2997.
- Lohr JG, Stojanov P, Carter SL, Cruz-Gordillo P, Lawrence MS, Auclair D, et al. Widespread genetic heterogeneity in multiple myeloma: implications for targeted therapy. *Cancer Cell*. 2014;25(1):91–101.
- Walker BA, Mavrommatis K, Wardell CP, Ashby TC, Bauer M, Davies FE, et al. Identification of novel mutational drivers reveals oncogene dependencies in multiple myeloma. *Blood*. 2018;132(6):587–97.
- Feng X, Guo J, An G, Wu Y, Liu Z, Meng B, et al. Genetic aberrations and interaction of NEK2 and TP53 accelerate aggressiveness of multiple myeloma. *Adv Sci (Weinh)*. 2022;9(9):e2104491.
- Tang X, Deng Z, Ding P, Qiang W, Lu Y, Gao S, et al. A novel protein encoded by circHNRNP1 promotes multiple myeloma progression by regulating the bone marrow microenvironment and alternative splicing. *J Exp Clin Cancer Res*. 2022;41(1):85.

9. Tirier SM, Mallm JP, Steiger S, Poos AM, Awwad MHS, Giesen N, et al. Subclone-specific microenvironmental impact and drug response in refractory multiple myeloma revealed by single-cell transcriptomics. *Nat Commun*. 2021;12(1):6960.
10. Wei R, Cui X, Min J, Lin Z, Zhou Y, Guo M, et al. NAT10 promotes cell proliferation by acetylating CEP170 mRNA to enhance translation efficiency in multiple myeloma. *Acta Pharm Sin B*. 2022;12(8):3313–25.
11. Bahls NJ. Darwinian evolution and tiding clones in multiple myeloma. *Blood*. 2012;120(5):927–8.
12. Dang M, Wang R, Lee HC, Patel KK, Becnel MR, Han G, et al. Single cell clonotypic and transcriptional evolution of multiple myeloma precursor disease. *Cancer Cell*. 2023;41(6):1032–47.e4.
13. Liang Y, He H, Wang W, Wang H, Mo S, Fu R, et al. Malignant clonal evolution drives multiple myeloma cellular ecological diversity and microenvironment reprogramming. *Mol Cancer*. 2022;21(1):182.
14. Mutational signatures across human cancer 2015 [Available from: https://cancer.sanger.ac.uk/signatures/signatures_v2/].
15. Alexandrov LB, Nik-Zainal S, Wedge DC, Aparicio SA, Behjati S, Biankin AV, et al. Signatures of mutational processes in human cancer. *Nature*. 2013;500(7463):415–21.
16. Manier S, Salem KZ, Park J, Landau DA, Getz G, Ghobrial IM. Genomic complexity of multiple myeloma and its clinical implications. *Nat Rev Clin Oncol*. 2017;14(2):100–13.
17. Talevich E, Shain AH, Botton T, Bastian BC. CNVkit: genome-wide copy number detection and visualization from targeted DNA sequencing. *PLoS Comput Biol*. 2016;12(4):e1004873.
18. Mermel CH, Schumacher SE, Hill B, Meyerson ML, Beroukhi R, Getz G. GISTIC2.0 facilitates sensitive and confident localization of the targets of focal somatic copy-number alteration in human cancers. *Genome Biol*. 2011;12(4):R41.
19. Sondka Z, Bamford S, Cole CG, Ward SA, Dunham I, Forbes SA. The COSMIC cancer gene census: describing genetic dysfunction across all human cancers. *Nat Rev Cancer*. 2018;18(11):696–705.
20. Lawrence MS, Stojanov P, Polak P, Kryukov GV, Cibulskis K, Sivachenko A, et al. Mutational heterogeneity in cancer and the search for new cancer-associated genes. *Nature*. 2013;499(7457):214–8.
21. Garcés JJ, Simicek M, Vicari M, Brozova L, Burgos L, Bezdekova R, et al. Transcriptional profiling of circulating tumor cells in multiple myeloma: a new model to understand disease dissemination. *Leukemia*. 2020;34(2):589–603.
22. Rodriguez-Otero P, Paiva B, San-Miguel JF. Roadmap to cure multiple myeloma. *Cancer Treat Rev*. 2021;100:102284.
23. Li GM. Mechanisms and functions of DNA mismatch repair. *Cell Res*. 2008;18(1):85–98.
24. Thibodeau SN, Bren G, Schaid D. Microsatellite instability in cancer of the proximal colon. *Science*. 1993;260(5109):816–9.
25. Yamamoto H, Imai K, Peruchio M. Gastrointestinal cancer of the microsatellite mutator phenotype pathway. *J Gastroenterol*. 2002;37(3):153–63.
26. Zhao P, Li L, Jiang X, Li Q. Mismatch repair deficiency/microsatellite instability-high as a predictor for anti-PD-1/PD-L1 immunotherapy efficacy. *J Hematol Oncol*. 2019;12(1):54.
27. Frerichs KA, Verkleij CPM, Dimopoulos MA, Marin Soto JA, Zweegman S, Young MH, et al. Efficacy and safety of daratumumab combined with daratumumab in daratumumab-refractory multiple myeloma patients. *Cancers (Basel)*. 2021;13(10):2452.
28. Mateos MV, Blacklock H, Schjesvold F, Oriol A, Simpson D, George A, et al. Pembrolizumab plus pomalidomide and dexamethasone for patients with relapsed or refractory multiple myeloma (KEYNOTE-183): a randomised, open-label, phase 3 trial. *Lancet Haematol*. 2019;6(9):e459–69.
29. Moreau P, Ghori R, Farooqui M, Marinello P, San MJ. Pembrolizumab combined with carfilzomib and low-dose dexamethasone for relapsed or refractory multiple myeloma: cohort 2 of the phase I KEYNOTE-023 study. *Br J Haematol*. 2021;194(1):e48–51.
30. Song W, Zhang M. Use of CAR-T cell therapy, PD-1 blockade, and their combination for the treatment of hematological malignancies. *Clin Immunol*. 2020;214:108382.
31. Ling J, Kumar R. Crosstalk between NFκB and glucocorticoid signaling: a potential target of breast cancer therapy. *Cancer Lett*. 2012;322(2):119–26.
32. Roche ME, Ko YH, Domingo-Vidal M, Lin Z, Whitaker-Menezes D, Birbe RC, et al. TP53 induced glycolysis and apoptosis regulator and monocarboxylate transporter 4 drive metabolic reprogramming with c-MYC and NFκB activation in breast cancer. *Int J Cancer*. 2023;153(9):1671–83.
33. Weniger MA, Küppers R. NF-κB deregulation in Hodgkin lymphoma. *Semin Cancer Biol*. 2016;39:32–9.
34. Yang W, Liu L, Li C, Luo N, Chen R, Li L, et al. TRIM52 plays an oncogenic role in ovarian cancer associated with NF-κB pathway. *Cell Death Dis*. 2018;9(9):908.
35. Godbersen JC, Humphries LA, Danilova OV, Kebbekus PE, Brown JR, Eastman A, et al. The Nedd8-activating enzyme inhibitor MLN4924 thwarts microenvironment-driven NF-κB activation and induces apoptosis in chronic lymphocytic leukemia B cells. *Clin Cancer Res*. 2014;20(6):1576–89.
36. Jani TS, DeVecchio J, Mazumdar T, Agyeman A, Houghton JA. Inhibition of NF-κappaB signaling by quinacrine is cytotoxic to human colon carcinoma cell lines and is synergistic in combination with tumor necrosis factor-related apoptosis-inducing ligand (TRAIL) or oxaliplatin. *J Biol Chem*. 2010;285(25):19162–72.
37. Cai H, Yan L, Liu N, Xu M, Cai H. IFI16 promotes cervical cancer progression by upregulating PD-L1 in immunomicroenvironment through STING-TBK1-NF-κB pathway. *Biomed Pharmacother*. 2020;123:109790.
38. Bernassola F, Karin M, Ciechanover A, Melino G. The HECT family of E3 ubiquitin ligases: multiple players in cancer development. *Cancer Cell*. 2008;14(1):10–21.
39. Swenson SA, Gilbreath TJ, Vahle H, Hynes-Smith RW, Graham JH, Law HC, et al. UBR5 HECT domain mutations identified in mantle cell lymphoma control maturation of B cells. *Blood*. 2020;136(3):299–312.
40. Gandolfi S, Laubach JP, Hideshima T, Chauhan D, Anderson KC, Richardson PG. The proteasome and proteasome inhibitors in multiple myeloma. *Cancer Metastasis Rev*. 2017;36(4):561–84.
41. Han X, Chen J, Wang J, Xu J, Liu Y. TTN mutations predict a poor prognosis in patients with thyroid cancer. *Biosci Rep*. 2022;42(7):BSR20221168.
42. Zheng QX, Wang J, Gu XY, Huang CH, Chen C, Hong M, et al. TTN-AS1 as a potential diagnostic and prognostic biomarker for multiple cancers. *Biomed Pharmacother*. 2021;135:111169.
43. Mao W, Zhou J, Hu J, Zhao K, Fu Z, Wang J, et al. A pan-cancer analysis of FAT atypical cadherin 4 (FAT4) in human tumors. *Front Public Health*. 2022;10:969070.
44. Li SS, Zhai XH, Liu HL, Liu TZ, Cao TY, Chen DM, et al. Whole-exome sequencing analysis identifies distinct mutational profile and novel prognostic biomarkers in primary gastrointestinal diffuse large B-cell lymphoma. *Exp Hematol Oncol*. 2022;11(1):71.
45. Zhu Q, Wang J, Zhang W, Zhu W, Wu Z, Chen Y, et al. Whole-genome/exome sequencing uncovers mutations and copy number variations in primary diffuse large B-cell lymphoma of the central nervous system. *Front Genet*. 2022;13:878618.
46. Chang H, Qi X, Yeung J, Reece D, Xu W, Patterson B. Genetic aberrations including chromosome 1 abnormalities and clinical features of plasma cell leukemia. *Leuk Res*. 2009;33(2):259–62.
47. Gowin K, Skerget S, Keats JJ, Mikhael J, Cowan AJ. Plasma cell leukemia: a review of the molecular classification, diagnosis, and evidenced-based treatment. *Leuk Res*. 2021;111:106687.
48. Greipp PR, San Miguel J, Durie BG, Crowley JJ, Barlogie B, Bladé J, et al. International staging system for multiple myeloma. *J Clin Oncol*. 2005;23(15):3412–20.
49. Palumbo A, Avet-Loiseau H, Oliva S, Lokhorst HM, Goldschmidt H, Rosinol L, et al. Revised international staging system for multiple myeloma: a report from international myeloma working group. *J Clin Oncol*. 2015;33(26):2863–9.
50. Guardia T, Eason M, Kontrogiani-Konstantopoulos A. Obscurin: a multitasking giant in the fight against cancer. *Biochim Biophys Acta Rev Cancer*. 2021;1876(1):188567.
51. Tuntithavornwat S, Shea DJ, Wong BS, Guardia T, Lee SJ, Yankaskas CL, et al. Giant obscurin regulates migration and metastasis via RhoA-dependent cytoskeletal remodeling in pancreatic cancer. *Cancer Lett*. 2022;526:155–67.
52. Guardia T, Zhang Y, Thompson KN, Lee SJ, Martin SS, Konstantopoulos K, et al. OBSCN restoration via OBSCN-AS1 long-noncoding RNA CRISPR-targeting suppresses metastasis in triple-negative breast cancer. *Proc Natl Acad Sci U S A*. 2023;120(11):e2215553120.

53. Dyson NJ. RB1: a prototype tumor suppressor and an enigma. *Genes Dev.* 2016;30(13):1492–502.
54. Yao Y, Gu X, Xu X, Ge S, Jia R. Novel insights into RB1 mutation. *Cancer Lett.* 2022;547:215870.

Publisher's Note

Springer Nature remains neutral with regard to jurisdictional claims in published maps and institutional affiliations.